Mon. Not. R. Astron. Soc. **000**, 000–000 (0000) Printed 16 February 2015 (MN LATEX style file v2.2)

Combining Spectroscopic and Photometric Surveys: Same or different sky?

Martin Eriksen[1,2], Enrique Gaztañaga[1]

[1]*Institut de Ciències de l'Espai (IEEC-CSIC), E-08193 Bellaterra (Barcelona), Spain*
[2]*Leiden Observatory, Leiden University, PO Box 9513, NL-2300 RA Leiden, Netherlands*

arXiv:1412.8429v2 [astro-ph.CO] 13 Feb 2015

16 February 2015

ABSTRACT

This article looks at the combined constraints from a photometric and spectroscopic survey. These surveys will measure cosmology using weak lensing (WL), galaxy clustering, baryon acoustic oscillations (BAO) and redshift space distortions (RSD). We find, contrary to some findings in the recent literature, that overlapping surveys can give important benefits when measuring dark energy. We therefore try to clarify the status of this issue with a full forecast of two stage-IV surveys using a new approach to properly account for covariance between the different probes in the overlapping samples. The benefit of the overlapping survey can be traced back to two factors: additional observables and sample variance cancellation. Both needs to be taken into account and contribute equally when combining 3D power spectrum and 2D correlations for lensing. With an analytic example we also illustrate that for optimal constraints, one should minimize the (Pearson) correlation coefficient between cosmological and nuisance parameters and maximize the one among nuisance parameters (e.g. galaxy bias) in the two samples. This can be achieved by increasing the overlap between the spectroscopic and photometric surveys. We show how BAO, WL and RSD contribute to this benefit and also look at some other survey designs, such as photometric redshift errors and spectroscopic density.

1 INTRODUCTION

The characteristics of a galaxy survey are in practice limited by time constraints. One can spend the time going deeper or overlapping different probes, or going wider. The issue of overlapping surveys has been an open question in the literature for the last few years. Several groups have been working on the topic, trying to find out if it is better to combine spectroscopic and photometric galaxy surveys on the same or different parts of the sky. Besides the benefit of finding an optimal design, these studies can also help in understanding the best way to combine different probes.

This paper proceeds a series of related papers by the same authors on this topic. The first deals with modeling of the correlation function. The second studies the relative impact of WL, RSD and BAO on cosmological forecast. The third focus on the impact of galaxy bias. From now, we will refer to these as paper-I(Eriksen & Gaztanaga 2014), paper-II(Eriksen & Gaztanaga 2015a) and paper-III(Eriksen & Gaztanaga 2015b). In this paper we focus on the combined constraints from a photometric and spectroscopic survey.

The combination of spectroscopic and weak lensing surveys helps to reduce the statistical errors on cosmological parameters (Bernstein & Cai 2011; Gaztañaga et al. 2012; Cai & Bernstein 2012; Kirk et al. 2013; Font-Ribera et al. 2013; de Putter et al. 2013). To a great extend the reduction comes from the complementarity (and independence) of the probes used in WL, RSD and BAO. That is something which can be done when combining two surveys over separate parts of the sky. In addition, overlapping surveys includes additional cross-correlations between the two galaxy samples which could in principle add or reduce the above benefits.

The galaxy density fluctuations follow the underlying dark matter fluctuations. This is something we can actually observe. There is also good agreement between the shape of the dark matter power spectrum and the galaxy power spectrum, or the corresponding 2D-correlations. These are related with a conversion factor called the galaxy bias b. The bias factor depends on how well the galaxies are tracing the underlying mass. This is again dependent on the galaxy types and magnitudes. Therefore, splitting or selecting galaxies will give samples with different characteristics.

These different galaxy probes are not independent because they trace the same underlying matter. However this can result in sample variance cancellation and reduce the errors on the cosmological parameters. A multiple tracer technique is a method already suggested in the literature to reduce sampling variance within a survey McDonald & Seljak (2009); Cai & Bernstein (2012); Asorey et al. (2014). In this article, the sampling variance can also cancel between

© 0000 RAS

the photometric and spectroscopic survey, between WL and RSD or galaxy counts of different galaxy types combination, as long as we are careful to include the full covariance between then. The relative impact of this cancellation will strongly depend on how much correlated are these probes relative to how much information there is in each separate measurement.

The first section in this paper introduces the forecast assumptions. These are already detailed in the other papers of these series, therefore the explanation is kept to a minimum. The second section presents the forecast of different survey configurations and probes, studying how these contribute to the benefit of overlapping galaxy surveys. In section three we present a generic analytical example to help interpreting the sample variance cancellation in the forecast. In the fourth section, we study how the galaxy density and redshift uncertainty affect the conclusions on overlapping surveys. We end with a conclusion.

2 FORECAST ASSUMPTIONS

In this section we briefly present the forecast assumptions, which corresponds directly to the setup in a series of papers (paper I, II, III). While the description here provide the most essential assumptions, the reader is referred to paper-II for more detailed information and discussion. A study of 2D-correlations in narrow bins can be found in paper-I.

Observables and Fisher forecast. The forecast study the combined constraints on dark energy and simple deviations from general relativity from intrinsic galaxy clustering, RSD and WL. A spectroscopic survey with excellent redshift information is ideal to measure RSD and intrinsic galaxy clustering, while a photometric survey allow for shape measurements to probe weak lensing. To simplify the survey combination, we analyze both surveys using 2D-correlations of galaxy count overdensities and galaxy shear. See paper-I for a detailed treatment.

We use the Fisher matrix formalism to propagate the covariance of observed correlations to the covariance (and errors) of the cosmological parameters. Let C_x be a 2D cross-correlation, with the index $x \equiv \{\ell, z_1, z_2, p_1, p_2\}$ being a combination of angular multipole scale ℓ, the two redshift bins (z_1, z_2) and galaxy populations (p_1, p_2). The Fisher matrix is then

$$F_{\mu\nu} = \sum_{x,y} \frac{\partial C_x}{\partial p_\mu} \left(Cov^{-1}\right)_{x,y} \frac{\partial C_y}{\partial p_\nu} \tag{1}$$

where Cov^{-1} is the inverse covariance between the observable and $\partial C_x/\partial p_\mu$ is the derivative with respect to a parameter μ. The double sum (x, y) is over all considered observables. Inverting the Fisher matrix,

$$Cov_{\mu\nu} = \left(F^{-1}\right)_{\mu\nu} \tag{2}$$

estimate the covariance of the parameters. While the Fisher matrix use a Gaussian approximation for the parameter likelihood and these errors are lower bounds, the Fisher matrices are a standard tool for cosmological forecast and can provide good physical insight.

Parameter	Photometric (F)	Spectroscopic (B)
Area [deg^2]	14,000	14,000
Magnitude limit	$i_{AB} < 24.1$	$i_{AB} < 22.5$
Redshift range	$0.1 < z < 1.5$	$0.1 < z < 1.25$
Redshift uncertainty	0.05(1+z)	0.001 (1+z)
z Bin width; # bins	0.07 (1+z); 12 bins	0.01(1+z); 71 bins
Bias: b(z)	1.2 + 0.4(z - 0.5)	2 + 2(z - 0.5)
Shape noise	0.2	No shapes
density [gal/arcmin^2]	6.5	0.4
nz - z_0	0.702	0.467
nz - α	1.274	1.913
nz - β	2.628	1.083

Table 1. Parameters describing the two surveys/populations. The first block give the area, magnitude limit, redshift range used in the forecast, redshift uncertainty modeled as a Gaussian and the redshift bin width. Second block give the galaxy bias ($\delta_g = b\delta_m$ and average galaxy shape uncertainty. Third block give the galaxy density and parameters for the n(z) shape.

Galaxy samples The forecast in 2D-correlations models the photometric (F for Faint) and spectroscopic (B for Bright) surveys as two galaxy populations. Forecasting the parameter errors depends on e.g. the redshift uncertainty, galaxy density and galaxy bias of both populations. For simplicity, the most important values are summarized in Table 1, while assumptions on minor effects (e.g. cosmic magnification) and plots can be found in paper-II. The galaxy densities follow the distributions

$$\frac{dN}{d\Omega dz} \propto (z/z_0)^\alpha \exp\left(-(z/z_0)^\beta\right) \tag{3}$$

with the parameters given in the last block of Table 1.

Since galaxies often occupy dense regions, the galaxy densities are biased ($\delta_g = b\delta_m$) with respect to the matter distribution. The bias factor, which depends both on galaxy formation and selection effects, is an important uncertainty in the combined forecast. When combining photometric and spectroscopic surveys, part of the gain comes from improving galaxy bias constraints. This forecast use one (linear) bias parameter for each redshift bin and galaxy population. Note that this is different from Gaztañaga et al. (2012), which used a smaller number of bias parameters. The fiducial bias evolution $b(z)$ for each population is given in Table 1.

Figure of Merit (FoM) A Figure of Merit compress the ability to measure cosmological parameters into a single number. While characterizing the full strength of a survey is more involved, it allows to simple compare the relative strength of surveys, probes and their combinations. To allow for both measuring the expansion and growth history, we define

$$\mathrm{FoM}_{w\gamma} \equiv \frac{1}{\sqrt{\det\left[\left(F^{-1}\right)_S\right]}} \tag{4}$$

where S the parameter subspace of w_0, w_a, γ, and therefore extends the DETF FoM by including the γ parameter, see

Gaztañaga et al. (2012). The forecast include Planck priors (see paper-II) and marginalizing over cosmological parameters $\Omega_m, \Omega_{DE}, \Omega_b, h, \sigma_8, n_s$ [1]. We also marginalize over bias parameters, which follows the fiducial relations in Table 1 with one bias parameter in each redshift bin, separate for each of the galaxy population. A detailed study of the galaxy bias can be found in paper-III.

Non-linear scales The forecast only use linear scales. In addition to $\ell_{max} = 300$, which for technical reasons is used for all correlations, we additionally remove correlations with too high $k = \ell/\chi(z)$ to prevent low redshift bins to enter into the non-linear regime. If either redshift bins in a correlations has $k > k_{max}(z) = \exp(-2.29 + 0.88z)$, the correlation is removed. For further details, see paper-II.

3 BENEFIT OF OVERLAPPING SURVEYS

This section present the main arguments of overlapping versus non-overlapping galaxy surveys. The first subsection present the forecast for different probes and the contribution of WL, RSD and BAO. The second subsection explains the contribution from galaxy clustering with multiple tracers and also from cross-correlations of galaxy counts with background shear. In the third section, we discuss the sampling variance cancellations that comes from overlapping surveys tracing the same matter fluctuations. Last subsection comments on how overlapping surveys also help to reduce systematic effects.

3.1 Increasing FoMs

Table 2 contains the main forecast table. The two first lines are respectively for overlapping and non-overlapping surveys, when including both galaxy counts and shear. The ratio line show the statistical benefit of having overlapping surveys. For the nominal survey, the $\mathrm{FoM}_{w\gamma}$ increase with 50% or equivalent 30% in the area. Further, one see that the result depends on the galaxy bias. Fixing the galaxy bias strongly increase the $\mathrm{FoM}_{w\gamma}$, but decrease the benefit of overlapping surveys. For a more detailed treatment, see paper-III.

Each column either fix the bias (second column) or remove a physical effect, while keeping the same correlations. Removing effects like doing the forecast in real space is unobservable, but it is shown to demonstrate the relative effects. Including WL, RSD and BAO respectively increase $\mathrm{FoM}_{w\gamma}$ with factors of 4.8, 2.1 and 1.3. This shows that both lensing and RSD are significant contributions. Also, while the forecast include the full power spectrum, the BAO is an important contribution. For a fixed bias or without lensing, the same-sky ratio drops. This happens because overlapping surveys better constrains the free bias parameters and without lensing there are no additional counts-shear ($\langle\delta\gamma\rangle$) cross-correlations. Instructively, the benefit without BAO and RSD show the competition between higher constraints in the separate surveys and the benefit of overlapping surveys. The second section in Table 2 shows the same results using only galaxy counts (no shear). Results are qualitative similar to the ones with shear, but the FoM are smaller, as expected.

To compare the combination of surveys (FxB, F+B) to the constraints to a single survey, Table 2 include F:All, B:All, F:Counts and B:Counts. The last two lines show the forecast when only using clustering of galaxy counts. Despite being deeper, the F sample has much lower $\mathrm{FoM}_{w\gamma}$ due to larger photo-z scatter. Constraints from galaxy clustering and RSD is therefore much higher in spectroscopic than photometric surveys. Also note how removing BAO (last column) reduce the $\mathrm{FoM}_{w\gamma}$ by less than half, while removing RSD has a much larger impact.

Weak lensing also affects the number counts through magnification. The impact is small for the spectroscopic survey where the RSD dominates. However, for the photometric (F) sample with only number counts, magnification increase $\mathrm{FoM}_{w\gamma}$ by 50%[2]. One should also note the difference between F:All, B:All and F+B:All. Even if the surveys are not overlapping, their combined constraints are much higher. This comes from WL and RSD probing different parameter combinations. Thus, one can greatly benefit from combining photometric and spectroscopic surveys, even when they do not overlap.

3.2 Counts-Shear cross-correlations

Overlapping surveys allow for the cross-correlation of the two samples. The important contributions are the cross-correlations of galaxy counts ($\langle\delta_F\delta_B\rangle$), which is a multi tracer approach and the correlations of spectroscopic galaxy counts with background shear $\langle\delta_B\gamma_F\rangle$. In this subsection we study the effect of counts-shear correlations ($\langle\delta\gamma\rangle$), which either comes from the cross-correlation of foreground spectroscopic galaxies ($\langle\delta_B, \gamma_F\rangle$) or from within the photometric population ($\langle\delta_F\gamma_F\rangle$).

The count-shear correlations contribute important information. While the auto-correlations, ignoring RSD, depend on b^2, the counts-shear correlations depend linearly on the bias (b). Measuring both the counts-counts auto-correlations and the count-shear cross-correlations leads to important improvements. The counts-shear correlations alone give weak bias constraints. The benefit comes from measuring the galaxy bias with galaxy clustering and then using these bias measurements to improve cosmological constraints from the counts-shear cross-correlations.

Section 4 of Table 2 investigates how the different counts-shear cross-correlations contribute. The three lines

[1] The fiducial forecast is a wCDM model, with values of cosmological parameters to match the MICE (www.ice.cat/mice) cosmological simulations. The densities of matter, dark energy and baryonic matter are respectively $\Omega_m = 0.25$, $\Omega_{DE} = 0.75$, $\Omega_b = 0.044$. For the dark matter power spectrum P(k), $\sigma_8 = 0.8$ is the amplitude of fluctuations in a 8Mpc/h sphere, while $P(k) = k^{0.95}$ on large scales. The dark energy component has an equation which equals a cosmological constant. In the forecast, we use the Eisenstein-Hu power spectrum model, which has the option of removing effects of BAO.

[2] In Gaztañaga et al. (2012) we used a different and more confusing notation. There "MAG", which equals what we now label "Counts", included both magnification and galaxy clustering.

Probe combinations	Fiducial	Fix Bias	No WL	No RSD	No BAO	Observables included
FxB:All	35.5	213	7.32	17.1	27.8	F+B:All + $\langle\delta_B\delta_F\rangle$ + $\langle\delta_B\gamma_F\rangle$
F+B:All	24.3	193	6.13	11.0	18.0	F:All + B:All
Ratio	1.5	1.1	1.2	1.6	1.6	(FxB/F+B):All
FxB:Counts	8.3	61.9	7.32	3.31	6.0	$\langle\delta_F\delta_F\rangle$ + $\langle\delta_B\delta_B\rangle$ + $\langle\delta_B\delta_F\rangle$
F+B:Counts	6.24	62.0	6.13	1.72	4.41	$\langle\delta_F\delta_F\rangle$ + $\langle\delta_B\delta_B\rangle$
Ratio	1.3	1.00	1.2	1.9	1.4	(FxB/F+B):Counts
F:All	3.10	51.2	0.06	2.61	2.77	$\langle\delta_F\delta_F\rangle$ + $\langle\delta_F\gamma_F\rangle$ + $\langle\gamma_F\gamma_F\rangle$
B:All	7.9	52.6	5.53	2.76	5.42	$\langle\delta_B\delta_B\rangle$ + $\langle\delta_B\gamma_B\rangle$ + $\langle\gamma_B\gamma_B\rangle$
F:Counts	0.08	2.85	0.06	0.04	0.05	$\langle\delta_F\delta_F\rangle$
B:Counts	5.53	45.4	5.53	1.45	3.78	$\langle\delta_B\delta_B\rangle$
FxB-$\langle\delta_F\gamma_F\rangle$:All	32.4	201	7.32	15.4	25.3	FxB:All - $\langle\delta_F\gamma_F\rangle$
FxB-$\langle\delta_B\gamma_F\rangle$:All	33.8	208	7.32	16.2	26.3	FxB:All - $\langle\delta_B\gamma_F\rangle$
FxB-$\langle\delta\gamma\rangle$:All	16.4	100	7.32	7.46	12.0	FxB:All - $\langle\delta_F\gamma_F\rangle$ - $\langle\delta_B\gamma_F\rangle$
FxB-$\langle$FB$\rangle$:All	30.7	199	6.05	14.1	23.3	F+B:All + Cov (same sky)
Ratio	1.3	1.0	0.99	1.3	1.3	(FxB-$\langle$FB$\rangle$/F+B):All
FxB-$\langle$FB$\rangle$:Counts	6.58	57.1	6.05	2.02	4.67	F+B:Counts + Cov (same sky)
Ratio	1.1	0.92	0.99	1.2	1.1	(FxB-$\langle$FB$\rangle$/F+B):Counts

Table 2. FoM$_{\gamma w}$ in units of 10^{-3}. Each row corresponds to a different combination of probes, including either counts δ and shear γ (All) or just galaxy counts (Counts). The combination FxB refers to the same sky case, while F+B is for separate sky for the photometric (F) and spectroscopic (B) samples. Block 3 of rows show the single population results. In block 4,5,6 or rows are the FxB case when removing some of the cross-correlations as observables, but keep the covariance from overlapping surveys. This is done for counts-shear ($-\langle\delta\gamma\rangle$) or from all cross-correlations between F and B samples (-$\langle$FB$\rangle$). On the columns is first the fiducial case, including all the effects. The next columms show the fixed galaxy bias (i.e. assumed that bias is known), no gravitational lensing effects, no redshift space distortions effects and no BAO peak. For "No BAO" the forecast is done without BAO wiggles in the Eisenstein-Hu power spectrum, while "No RSD" use correlations in real space.

corresponds to FxB:All including different counts-shear correlations. In FxB-$\langle\delta_F\gamma_F\rangle$, FxB-$\langle\delta_B\gamma_F\rangle$ and FxB-$\langle\delta\gamma\rangle$, respectively the Faint-Faint, Bright-Faint and all count-shear cross-correlations are not included.

Removing either the $\langle\delta_F\gamma_F\rangle$ or $\langle\delta_B\gamma_F\rangle$ cross-correlations has less than 7% effect on the overall constraints. However dropping both count-shear cross-correlations reduce the constraints with 52%. One should be careful and include all counts-shear cross-correlations in the forecast. Including counts-shear cross-correlations for the overlap ($\langle\delta_B\gamma_F\rangle$), but ignoring the information for the photometric population alone ($\langle\delta_F\gamma_F\rangle$), will overestimate the same-sky benefit. We expect this is the main difference to the findings of Kirk et al. (2013).

3.3 Reduced sample variance

Besides additional cross-correlations, overlapping volumes directly reduce the cosmic variance. When two surveys overlap the same volume, the galaxy overdensities trace the same underlying matter fluctuations. Measuring the same fluctuations with covariant observables helps in measuring the underlying matter densities. This multi-tracer technique is a well known method to reduce the sampling variance (McDonald & Seljak 2009; Asorey et al. 2012; Cai & Bernstein 2012).

Last section in Table 2 quantify the benefit of overlapping volumes. The forecast of overlapping surveys (FxB) include covariance between the samples, while the non-overlapping surveys (F+B) are considered independent. The line FxB-$\langle$FB$\rangle$ provide a case in-between FxB and F+B, where the surveys overlap, but without including (as observables) the additional cross-correlations between the surveys. Thus the only difference between FxB-$\langle$FB$\rangle$ and F+B is including the covariance between the samples (B and F) in FxB-$\langle$FB$\rangle$. Naively one expect a lower FoM$_{w\gamma}$ from FxB-$\langle$FB$\rangle$ than from either FxB or F+B, since the covariance often reduce the available information.

Including the covariance increase the fiducial FoM$_{w\gamma}$ by 26% (see (FxB-$\langle$FB$\rangle$/F+B):All), while the effect is only 3% for a fixed galaxy bias. This shows the additional covariance from overlapping surveys, increase the FoM$_{w\gamma}$ through better bias constraints. For counts alone the increase is smaller. When bias is known, the additional covariance in the counts reduce, rather than increase, the FoM. When also including shear, the bias can also be measured from $\langle\delta_F\gamma_F\rangle$, which explains additional benefits in (FxB-$\langle$FB$\rangle$/F+B):All than with the Counts alone.

A different forecast method to the 2D-correlations used here, is to combine the spectroscopic 3D power spectrum and the 2D counts-shear and shear-shear correlations, see Gaztañaga et al. (2012)[3]. When combining a 3D and 2D

[3] In Gaztañaga et al. (2012) the FxB and F+B notation did not correspond directly to overlapping and non-overlapping surveys. Instead F+B was the traditional use of photometric and spectroscopic surveys, while FxB combined the surveys over the same area and also used the photometric sample to measure RSD.

forecast, one needs to include the covariance between the 2D and 3D estimator. The forecast will otherwise not properly include sample variance cancellation and be biased towards a lower same-sky benefit. Not properly including the covariance can partially explain why Font-Ribera et al. (2013) and de Putter et al. (2013) find lower benefit from overlapping surveys. These analysis separate use a 2D correlation for the transverse modes and a 3D power spectrum for the rest. As the transverse component accounts for less than 6% of the modes (according to their own accounting), they ignore most of the covariance between the galaxy counts in the photometric and specroscopic sample.

These analysis differs in detail. The parameters included are different, since our analysis (in this paper) always marginalising over the growth index (γ), while others marginalise over the neutrino mass, but often fix the growth. Also the 2D+3D estimation ignore the radial information in the cross-correlations between the photometric and spectroscopic sample. For the 2D analysis in narrow bins, this effect give a significant contribution to the correlations (see paper-I). On the other hand, Font-Ribera et al. (2013) and de Putter et al. (2013) use $l_{max} = 2000$ for WL (and also larger k_{max} for BAO), which can reduce the overlap in Fourier space and reduce the same-sky benefit. We leave modelling the non-linear bias and extending out analysis to small scales for future work.

3.4 Control systematics

This paper focus on the statistical benefit of overlapping surveys. In addition, and potentially more important, the overlapping surveys provide other venues for reducing the impact of systematic errors. Examples include measuring the cross-correlations to reduce the uncertainty in the photometric galaxy redshift distribution (Newman 2008; Matthews & Newman 2010; Gaztañaga et al. 2012).

An frequently used approach to handle systematic errors is to parameterize the unknown quantity, e.g. the galaxy bias. This can remove systematic effects at the cost of increasing statistical errors. Additional parameters be physically motivated or selected to follow a mathematical model, e.g. linear in redshift. In both cases, the cross-correlations can help to constrain these parameters. One example is the stochastic bias model introduced in paper-III. When introducing a stochastic bias parameter, the overlapping surveys are less affected than non-overlapping surveys. We expect similar behavior might apply also to other forms of systematics.

4 A SIMPLE EXAMPLE

Stronger constraints from a higher covariance between observable might seen counter intuitive. This section illustrate why covariance can contribute positively when marginalizing over the galaxy bias.

Combined with problems with the RSD calculations, in particular underestimating the photo-z effect, this lead to overestimating the same-sky benefit.

4.1 Increased errors

The covariance matrix for two observables is

$$Cov = \begin{bmatrix} \sigma_1^2 & k\sigma_1\sigma_2 \\ k\sigma_1\sigma_2 & \sigma_2^2 \end{bmatrix} \tag{5}$$

where σ_1 and σ_2 are their errors. The factor k give the cross correlation (Pearson coefficient) between the observables, with $k = 0$ being independent and $k = 1$ fully correlated. Assuming the two observables are equal, the expected error of x (σ_x) estimated with a Fisher matrix is

$$\sigma_x^2 = \left(\frac{\sigma_O}{\partial O/\partial x}\right)^2 \left[\frac{k+1}{2}\right] \tag{6}$$

where σ_O is the error of the observables. Here uncorrelated ($k = 0$) observables produce the smallest errors, while the limit of fully correlated observables ($k = 1$) is the constraints from one observable alone. If O_1 and O_2 are the same observable measured from two surveys, then k is the fractional overlap in survey areas, ignoring observational noise.

4.2 General covariance - 3 parameters

The effect of a covariance changes when introducing nuisance parameters. Consider the general case of one cosmology parameter (P) and two nuisance parameters (1, 2). These could be the amplitude of fluctuations ($P = A$) and the two bias parameters (b_1, b_2) from different galaxy samples. Their Fisher matrix can be written

$$F = \begin{bmatrix} d_P^2 & r_{P1}\, d_P d_1 & r_{P2}\, d_P d_2 \\ r_{P1}\, d_P d_1 & d_1^2 & r_{12}\, d_1 d_2 \\ r_{P2}\, d_P d_2 & r_{12}\, d_1 d_2 & d_2^2 \end{bmatrix} \tag{7}$$

where d_i^2 is the diagonal component for parameter i. The off diagonal components ($r_{ij} d_i d_j$) are defined so $-1 \le r_{ij} \le 1$ are the Pearson correlation coefficient. For non-overlapping surveys, then $r_{12} = 0$ because observables including the two nuisance parameters are independent. A Fisher matrix can estimate the expected parameters variance $\sigma_i^2 = (F^{-1})_{ii}$ when marginalizing over the uncertainty in the other parameters. For the parameters P, the variance is

$$\sigma_P^2 = \frac{1}{d_P^2}\left[1 - \frac{r_{P1}^2 + r_{P1}^2 - 2 r_{P1}\, r_{P2}\, r_{12}}{1 - r_{12}^2}\right]^{-1} \tag{8}$$

where the requirement

$$r_{P2}^2 + r_{P1}^2 - 2 r_{P1} r_{P2} r_{12} \le 1 - r_{12}^2 \tag{9}$$

avoid negative values of the variance. From Eq. 8, the optimal error is $\sigma_A = 1/d_P$, which occurs when there is no covariance between P and the nuisance parameters ($r_{P1} = r_{P2} = 0$) . Further, decreasing either r_{P1} or r_{P2} will lead to better constrains on P. For $\alpha \equiv r_{p1} = r_{p2}$ the expected error on P (Eq.8) is

$$\sigma_P^2 = \frac{1}{d_P^2}\left[1 - \left(\frac{2\alpha^2}{1 + r_{12}}\right)\right]^{-1} \tag{10}$$

A larger r_{12} or smaller α reduce the error (and vice versa).

For optimal constraints, one should minimize the correlation between cosmology and the nuisance parameters (α), while maximizing the correlation between the nuisance parameters of the two samples (r_{12}). We have run some analytical examples of this and found that, as expected, r_{12} is proportional to k while alpha depends more weekly on k. This explains how the error in cosmological parameters could reduce as we increase the overlap between the two surveys (and therefore k).

4.3 General covariance - n parameters

The example can be extended to more parameters. Consider the Fisher matrix where the parameters are divided into the parameters of interest (p) and nuisance parameters (n). The covariance matrix is the by block inversion

$$F^{-1} = \begin{bmatrix} F_{pp} & F_{pn} \\ F_{np} & F_{nn} \end{bmatrix}^{-1} \tag{11}$$

$$= \begin{bmatrix} S_{nn}^{-1} & -F_{pp}^{-1}F_{pn}S_{pp}^{-1} \\ -F_{nn}^{-1}F_{np}S_{nn}^{-1} & S_{pp} \end{bmatrix} \tag{12}$$

where F_{xy} denote the Fisher matrix subspace for parameter sets x and y and the Schur complements (S_{nn}, S_{pp}) are defined by

$$S_{nn} \equiv F_{pp} - F_{pn}F_{nn}^{-1}F_{np} \tag{13}$$

$$S_{pp} \equiv F_{nn} - F_{np}F_{pp}^{-1}F_{pn}. \tag{14}$$

.

Equivalent to the general FoM_S (Gaztañaga et al. 2012), for which $\mathrm{FoM}_{w\gamma}$ (Eq. 4) is a special case, one have

$$\mathrm{FoM} \equiv \frac{1}{\sqrt{\det\left[(F^{-1})_{pp}\right]}} = \sqrt{\det\left[F_{pp} - F_{pn}F_{nn}^{-1}F_{np}\right]} \tag{15}$$

from Eq. 12 and 13. The FoM increase with higher correlation between nuisance parameters (in F_{nn}) and lower correlation between nuisance parameters and parameters of interest (F_{np}). Notice how the cosmological parameters marginalised over is included in the set of nuisance parameters (n). While the results also depend on the eigenvectors directions, but we are not discussing this here.

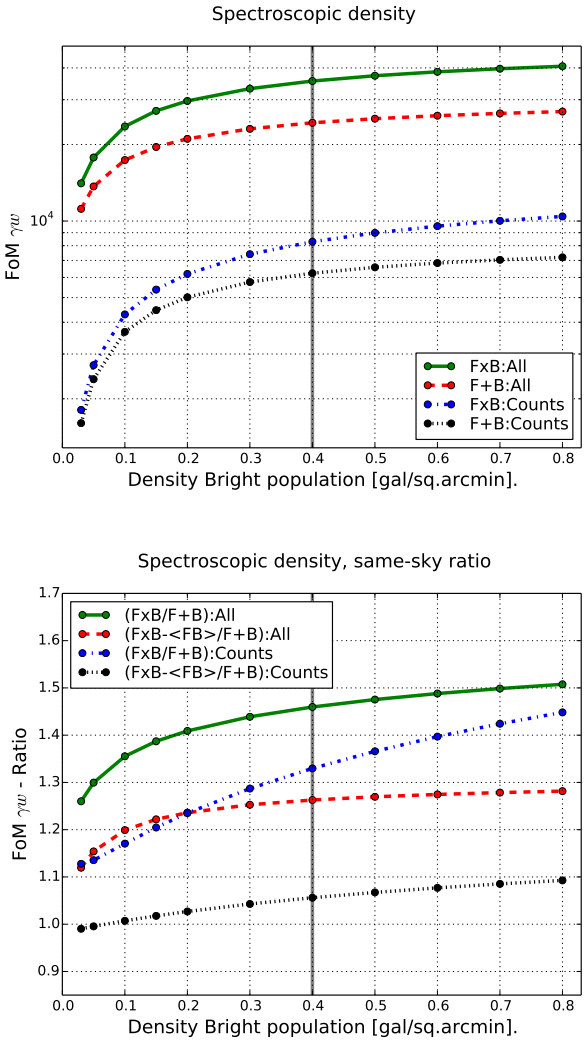

Figure 1. Effect of galaxy density in the spectroscopic sample. The top panel show the absolute $\mathrm{FoM}_{w\gamma}$, with the galaxy density on the x-axis and the four lines corresponds to FxB-All, F+B-All, FxB-Counts and F+B-Counts. A vertical line at 0.4 gal/sq.arcmin marks the fiducial spectroscopic galaxy density. In the lower panel, the ratios show the same-sky benefit (FxB/F+B) and the effect of the overlapping volumes (FxB-$\langle$FB$\rangle$/F+B).

5 SURVEY CONFIGURATIONS

The benefit of overlapping surveys depend on the survey specifications. We find a same-sky benefit over a wide range of configuration. However the exact benefit depend on details and need to be considered when comparing results in the literature. The combined forecast depends stronger on parameters of the spectroscopic survey. In this section, we therefore study the effect of spectroscopic density and the importance of radial information.

5.1 Spectroscopic galaxy density

The number of galaxies is a discrete quantity, which leads to a shot-noise term in the auto-correlation of galaxy overdensities. A higher spectroscopic density will reduce the measurement errors and increase the constraints on cosmology. But for a fixed survey time, there is a trade off between depth (longer exposures) and area covered. This subsection ignore survey optimization and study how increased densities improve constraints for a fixed area.

Fig. 1 shows the effect of increasing the galaxy density in the spectroscopic sample. For low densities, the configurations which only include galaxy counts (FxB-Counts, F+B-Count) drops drastically since the spectroscopic galaxy clustering dominates the constraints. Naturally, the effect is smaller when also including WL shear (FxB-All, F+B-All), because the lensing constraints primarily come from the photometric sample. The lines grow monotonically and flattens around 0.4 gal/sq.arcmin. Beyond this density, we only find small improvements by targeting higher densities. This turnover is affected by the removal of non-linear scales and the lmax value.

The bottom panel (Fig. 1) show the same-sky ratio. For low densities, the error is dominated by shot-noise and sample variance cancellation becomes less important. Therefore we find that the ratio increase with density. Also, the (FxB/F+B):Counts ratio grows faster because the spectroscopic density (B) affects the galaxy counts clustering more than the WL.

5.2 Redshift uncertainties

Spectroscopic galaxy surveys typically has excellent redshift determination. The Gaussian spectroscopic errors we assume ($\sigma_z = 0.001(1+z)$) are 50 times better than the photo-z errors ($\sigma_z = 0.05(1+z)$). This precision allows us to measure the radial information in the galaxy clustering. For this series of papers, the analysis is done with 2D cross-correlations in narrow redshift bins. The radial information is encoded in the intrinsic cross-correlations between the redshift bins (see paper-I, paper-II). This subsection forecasts the constraints for larger redshift errors for the spectroscopic (Bright) sample. Although the errors are artificially high, the results help to understand the benefit of high radial resolution.

Fig. 2 (top panel) shows $\mathrm{FoM}_{w\gamma}$ for increasing redshift uncertainties in the spectroscopic sample. Larger photo-z errors dramatically decrease the performance. The vertical line indicate the forecast for a narrow-band survey, e.g. PAU (Martí et al. 2014). For the fiducial redshift binning, the narrow-band photo-z error provide comparable constraints to a fully spectroscopic survey. This result depend on the redshift bin width. Thinner bins are more sensitive to the photo-z value, with details provided in paper-II. For larger errors of $\sigma_z = 0.05(1+z)$, the information in the galaxy clustering (Counts) drop by almost two orders of magnitude. This decrease is likely overestimated because the number of bins is fixed[4], but it demonstrates how the 2D-correlations in narrow bins benefit from the good redshift information.

The bottom panel (Fig. 2) shows the same-sky benefit ratio (FxB/F+B). When increasing the redshift uncertainties above $\sigma_{68} \approx 0.015(1+z)$, the ratios decline both for All and Counts. Including lensing allows measuring counts-shear from either spectroscopic or photometric foreground galaxies. This measurement depends on knowing the bias of the foreground galaxies. Higher redshift uncertainties directly increase the spectroscopic (B) bias error, while indirectly for the photometric (F) bias from cross-correlation of galaxy counts in the two samples. For only galaxy count, the weaker importance of Bright-Faint cross-correlations is partly compensated by a loss in spectroscopic bias (in F+B), but the same-sky ratio still declines. Two lines (FxB-$\langle$FB$\rangle$/F+B) show the direct benefit from overlapping volume. The (FxB-$\langle$FB$\rangle$/F+B):All ratio decline fast, which means the sampling variance cancellation is more dependent on good redshift resolution in the spectroscopic sample.

[4] We have 71 bins and bias parameters for the spectroscopic sample regardless of the photo-z uncertainties.

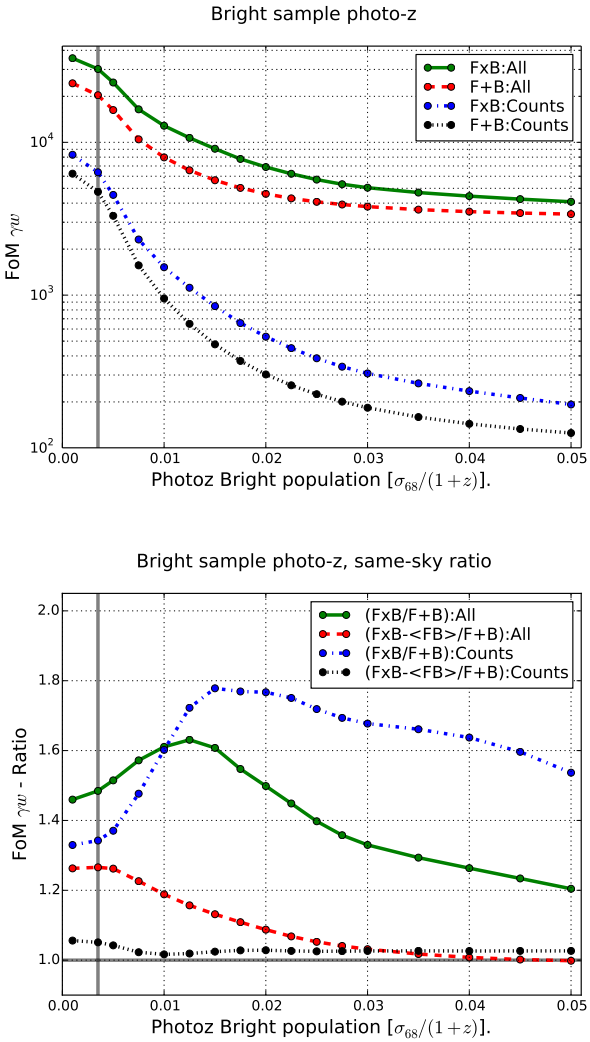

Figure 2. Impact of redshift errors of the Bright/spectroscopic galaxy sample. The top-panel show $\mathrm{FoM}_{w\gamma}$ increasing a Gaussian photo-z in the Bright/spectroscopic sample, with four lines corresponding to FxB-All, F+B-All, FxB-Counts and F+B-Counts. A vertical line at $\sigma_z = 0.0035(1+z)$ marks the expected photo-z in a narrow-band photometric survey. The lower panel shows the same-sky ratios and also including two ratios for the volume effect.

6 CONCLUSIONS

In a series of articles (paper-I, II and III) we have looked at at combining the information from photometric and spectroscopic surveys. The photometric surveys measures galaxy shapes and can constrain cosmology from weak gravitational lensing, while the accurate redshift determination in spectroscopic surveys is suited for galaxy clustering, RSD and BAO. A central question is: Should spectroscopic and photometric surveys ideally be over the same area? Previous studies disagree, finding either none or very high same-sky benefit. This paper summarized our understanding, building on the detailed study in paper-I, II and III.

Section 2 describe the forecast assumptions (for more details see paper-II). The weak lensing and galaxy counts are both analyzed using 2D-correlations, with narrow bins

in the spectroscopic sample. Radial information of the spectroscopic sample is included through intrinsic correlation between narrow redshift bins (see paper-I, paper-II, Asorey et al. (2012), Asorey et al. (2014)). The difference between overlapping (FxB) and non-overlapping (F+B) surveys is the additional cross-correlations and the additional covariance since both surveys trace the same matter fluctuations. We forecast the constraints using Fisher matrices, focusing on a combined figure of merit ($\mathrm{FoM}_{w\gamma}$), which includes w_0, w_a and the growth parameter γ. Note that all assumptions exactly match paper-I, II and III. The general ideas are the same as Gaztañaga et al. (2012), but the implementaion is quite different.

The $\mathrm{FoM}_{w\gamma}$ is estimated for the photometric (F) and spectroscopic (B) surveys alone and when combining them for overlapping (FxB) and non-overlapping (F+B) surveys. We consider only including galaxy counts, the effect of removing counts-shear cross-correlations and a special case to discuss the effect of overlapping volumes. All those cases are estimated when fixing the bias or ignoring the effect of WL, RSD or BAO. For the fiducial case (first row, first column in Table 2), we find overlapping surveys benefit 50% in $\mathrm{FoM}_{w\gamma}$ and equivalently 30% increase when only including galaxy counts.

One difference between overlapping and non-overlapping surveys are the additional cross-correlations. In the overlapping surveys, one can cross-correlate the foreground spectroscopic galaxy counts with the background shear. Including counts-shear is possible using either foreground photometric or spectroscopic galaxy counts. As presented in the main table, dropping either set of cross-correlations give a small change, while dropping both dramatically decrease the constraints. The benefit of additional correlations mainly comes from counts-counts cross-correlations, which constrains bias and therefore make the counts-shear more powerful. In Kirk et al. (2013) the authors acknowledge the strength of counts-shear in the photometric (F) sample, but ignore them in the combined forecast for technical reasons (private communication). This artificially increase the same-sky (FxB/F+B) benefit and probably explain most of the difference to our more modest same-sky benefit.

Overlapping surveys also directly improve constraints from the added covariance. The galaxy over-densities in both surveys trace the same underlying mass and the covariance leads to sample variance cancellations. Through a special case (FxB-$\langle$FB$\rangle$) which can be though as either removing all cross-correlations (between F and B) from FxB or adding covariance to the non-overlapping (F+B) surveys, we find about equal benefit from sample variance cancellation and the additional cross-correlations. In section 4, we demonstrate the non-intuitive effect of stronger covariance giving better cosmological constraints using a simplified analytical example. We show that for optimal constraints, one should minimize the correlation (Pearson coefficient) between cosmological and nuisance parameters and maximize the covariance between the nuisance parameters between the spectroscopic and photometric surveys, which is achieved by increasing the overlap between the two samples.

Previous analysis (Font-Ribera et al. 2013; de Putter et al. 2013) combined a 3D power spectrum of galaxy counts with 2D correlations for lensing, following Gaztañaga et al. (2012). These analysis ignore the (radial) covariance between the 2D and 3D estimator. Since the covariance between different tracers reduce the sample variance, ignoring this covariance could partially explain their lower benefit of overlapping surveys. These papers also ignore the significant radial information in the cross-correlation of the photometric and spectroscopic survey (paper-I). The assumptions also differs, including this paper using $l_{max} = 300$ for both WL and Counts, while two papers combining 2D and 3D use $l_{max} = 2000$ for WL and a larger k_{max} for BAO, which might affect the same-sky conclusion. Extending the forecast to non-linear scales is left to future work.

Section 5 looked at the impact of galaxy density and redshift errors. Starting from low galaxy densities in the B (spectroscopic) sample, increasing the density strongly improves the $\mathrm{FoM}_{w\gamma}$. This benefit saturate around 0.4 gal/sq.arcmin. for all considered configurations. The shot-noise from low densities decrease the benefit of sample variance cancellation. Increasing the densities therefore rise the same-sky ratio and the biggest change occurs when only galaxy counts are included. The last subsection investigated the dependence on accurate redshift errors in the spectroscopic sample. Through artificially increasing the spectroscopic redshift uncertainty, we find a strong degradation in constraints as a function of redshift accuracy.

In summary, this paper finds important gains from overlapping galaxy surveys. The statistical benefit comes from both additional cross-correlations and sample variance cancellations when using photometric and spectroscopic tracers. We have studied the literature and believe we could plausibly explain the discrepancies and confusion which is still surrounding the topic of overlapping galaxy surveys. We also identify several effects that impact this result and show an analytical example for the covariance from the overlapping surveys. In addition to reducing the statistical errors, the overlapping surveys can help reducing systematic uncertainties, which is needed for the next generation of galaxy surveys.

ACKNOWLEDGMENTS

We would like to thank the group within the DESI community looking at overlapping surveys. M.E. wish to thank Ofer Lahav, Henk Hoekstra and Martin Crocce in his thesis examination panel, where these results were discussed. E.G would like to thank Pat McDonald for exploring and comparing results. Funding for this project was partially provided by the Spanish Ministerio de Ciencia e Innovacion (MICINN), project AYA2009-13936 and AYA2012-39559, Consolider-Ingenio CSD2007- 00060, European Commission Marie Curie Initial Training Network CosmoComp (PITN-GA-2009-238356) and research project 2009- SGR-1398 from Generalitat de Catalunya. M.E. was supported by a FI grant from Generalitat de Catalunya. M.E. also acknowledge support from the European Research Council under FP7 grant number 279396.

REFERENCES

Asorey J., Crocce M., Gaztañaga E., 2014, MNRAS, 445,

2825
Asorey J., Crocce M., Gaztañaga E., Lewis A., 2012, MNRAS, 427, 1891
Bernstein G. M., Cai Y.-C., 2011, MNRAS, 416, 3009
Cai Y.-C., Bernstein G., 2012, MNRAS, 422, 1045
de Putter R., Doré O., Takada M., 2013, ArXiv e-prints, 1308.6070
Eriksen M., Gaztanaga E., 2014, ArXiv e-prints, (paper I) 1412.2208
Eriksen M., Gaztanaga E., 2015a, (paper II) In preparation
Eriksen M., Gaztanaga E., 2015b, (paper III) In preparation
Font-Ribera A., McDonald P., Mostek N., Reid B. A., Seo H.-J., Slosar A., 2013, ArXiv e-prints, 1308.4164
Gaztañaga E., Eriksen M., Crocce M., Castander F. J., Fosalba P., Marti P., Miquel R., Cabré A., 2012, MNRAS, 422, 2904
Kirk D., Lahav O., Bridle S., Jouvel S., Abdalla F. B., Frieman J. A., 2013, ArXiv e-prints, 1307.8062
Martí P., Miquel R., Castander F. J., Gaztañaga E., Eriksen M., Sánchez C., 2014, MNRAS, 442, 92
Matthews D. J., Newman J. A., 2010, ApJ, 721, 456
McDonald P., Seljak U., 2009, J. Cosmology Astropart. Phys., 10, 7
Newman J. A., 2008, ApJ, 684, 88